

Dynamic Coherence in Excitonic Molecular Complexes under Various Excitation Conditions

Aurélia Chenu,¹ Pavel Malý,¹ and Tomáš Mančal¹

¹*Faculty of Mathematics and Physics, Charles University in Prague,
Ke Karlovu 5, 121 16 Prague 2, Czech Republic*

In this paper, we investigate the relevance of dynamic electronic coherence under conditions natural to light-harvesting systems. We formulate the results of a quantum mechanical treatment of a weak light-matter interaction in terms of experimental observable, such as the incident light spectrum and the absorption spectrum of the material, and we derive the description of the incoherent Förster type energy transfer fully from the wave function formalism. We demonstrate that excitation of a coherent superposition of electronic eigenstates of natural light-harvesting complexes by sunlight or by excitation transfer from a neighboring antenna is unlikely and that dynamical coherence therefore cannot play any significant role in natural photosynthesis, regardless of their life time. Dynamical coherence as a transient phenomenon must be strictly distinguished from the effect of excited state delocalization (also termed quantum coherence in the literature) which is established by interaction between the pigments and is therefore a property of the system.

I. INTRODUCTION

Ever since the observation of long-lived oscillations in the two-dimensional (2D) spectra of a photosynthetic Fenna-Matthews-Olson (FMO) pigment-protein complex (PPC) and their interpretation as a signature for long-lived superposition of the electronic eigenstates of the complex, this effect (termed electronic quantum coherence) has been posited to play a significant role in achieving the remarkably high efficiency of electronic energy transfer (EET) in photosynthesis in general. Excited state delocalization, also often termed electronic quantum coherence, has been since long time ago known to play a significant role in the energy transport properties of molecular aggregates and molecular crystals (e.g. [1–4]). Delocalization of the electronic eigenstates over more than one pigment results from correlations between electrons of different pigments in the same molecular crystal or aggregate – which is mediated by direct electrostatic interaction, often simulated successfully by dipole-dipole interaction. Recently, the term quantum coherence has been consistently applied to quantum beats between electronic eigenstates in excited state band, which is a related but nevertheless distinct phenomenon. The quantum beats of this type were first observed spectroscopically in time resolved spectra of the FMO complex [5, 6]. Similar oscillations have been since then observed in other photosynthetic complexes such as the reaction center (RC) of a purple bacteria [7], the light-harvesting complex II (LHCII) from higher plants [8, 9], from marine algae [9, 10] and from purple bacteria [11] at room temperature (RT), as well as in conjugated polymers [12]. Table I presents the measured life times of the observed quantum beats in the different photosynthetic complexes. These oscillations have been mostly interpreted as a signature of superposition of electronic eigenstates. While in some cases, their life time is only few hundreds of femtoseconds [10, 11, 13], several photosynthetic complexes exhibit surprisingly long-lived oscillations [6–8, 13–15]. Theoretical

calculations assuming an electronic origin of the observed coherence also usually predict short life times or at least shorter than those observed in the experiment [16–18]. The main mechanism currently suspected to extend the life time of electronic coherence assumes spatial correlation between environmental degrees of freedom (DOF) of different pigments [7, 19–27]. Alternative explanations suggest the long-lived coherences to originate from interferences between different quantum pathways [28, 29] or from resonance coupling between the electronic and vibrational states [30–32].

The observation of quantum beating in various complexes seems to suggest that this is a general phenomenon in photosynthetic systems. But whether these effects are of importance for the high efficiency of photosynthesis or whether they are just artifacts of the ultra fast excitation used in laboratory situation remains a disputed question. As inferred by the authors from the current debate, it is often assumed that this coherence plays an essential role in light-harvesting efficiency. Such an assumption rests on the notion that a time dependent effect similar to the one observed in time-resolved experiments with ultra fast pulses accompanies light-harvesting of natural Sun light. Suggestions have been made that a thermal source consists of a collection of random femtosecond pulses, and that the experimental observations would be representative of the *in vivo* conditions [33]. However, based on both semi-classical and fully quantum mechanical representation of the light-matter interaction, it has been demonstrated that excitation by incoherent light as well as by one-photon absorption leads to a stationary mixed state and cannot create a superposition of energy eigenstates (*i.e.* dynamical coherence), neither on isolated molecules [34, 35] nor on open systems [36, 37]. Thereby, the existence of quantum coherence has been shown to be dependent on the excitation process [35, 36], which is in contrast with a qualitative description suggesting that the absorption of a single photon triggers the same coherent molecular response, regardless of the character of

the light source [38].

The aim of this paper is to consider the creation of dynamical coherences in a light-harvesting system in its natural conditions. In Section III we will extend the treatment of Ref. [36] to express the state of a molecular system weakly perturbed by stationary light to include the experimentally observable quantity, the light spectrum. Needless to say, this fully quantum mechanical treatment does not predict any time dependent coherences to be present after stationary light excitation. The other situation where it is often assumed that ultra fast discrete events occur, which would in principle lead to dynamical coherences on a single antenna level, is a focus of Sections IV and V. This situation is represented by the energy transfer between antennae. When dynamical coherence decays, the energy transfer does not stop, but rather proceeds in incoherent fashion. This is often referred to as incoherent or classical hopping. We will try to demonstrate in Section IV that strictly quantum mechanical treatment of this situation does not predict any

actual hopping in the incoherent mode of transfer. We will demonstrate in Section V that the condition for creation of a dynamical coherence by energy transfer from one antenna to another is very similar to the condition for creation of a coherence by pulsed light: the excitation has to occur ultra fast in a well defined time. Because the energy transfer times between the antennae in the system most prominent in the quantum biology discussions – chlorosome-FMO-reaction center system – are of the order of one picosecond or longer, we are lead to the conclusion that even if the FMO antenna were excited by a single excitation arriving at a well defined time at the chlorosomal base plate, and no decohering influence of the protein environment would be present, the FMO antenna would still demonstrate only a minor amount of coherence. Summarizing our results we conclude in Section VI that the answer to the question of efficiency of a (undoubtedly quantum) natural light-harvesting antennae does depend on the presence of dynamical coherence.

Measured system	Exp. tech.	Temp.	Life time
FMO (<i>Chlorobium tepidum</i>)	2D ES	77 K	>660 fs [6]
		277 K	>300 fs [14]
		77 K	>1800 fs [15]
RC (<i>Rhodobacter Sphaeroides</i>)	2CECPE	77 K	440 fs [7]
		180 K	310 fs [7]
LHCII (<i>Rhodobacter Sphaeroides</i>)	2D ES	RT	400 fs [11]
LHCII (purple bacteria)	ARC WM	RT	> 2800 fs [9]
LHCII (<i>Arabidopsis Thaliana</i>)	2D ES	77 K	>500 fs [8]
PC645 and PE545 (marine cryptophytes)	2D PES	294 K	>130 fs [10, 13]

Table I: Characteristic of the observed quantum beats in the various photosynthetic systems. 2DES stands for 2D Electronic Spectroscopy, 2DPES for 2D Photo Echo Spectroscopy, 2CECPE for Two-Color Electronic Coherence Photon Echo experiment and ARC WC for angle-resolved coherent wave mixing.

II. THEORETICAL DESCRIPTION OF LIGHT-HARVESTING ANTENNAE

In this section, we introduce the basics of the theoretical description for the photosynthetic PPCs and their internal energy transfer. We define more precisely what is meant by coherence (in singular) and coherences (in plural) and how they are related to the two distinct phenomena of exciton delocalization and dynamical quantum coherence.

A. Molecular Excitons and System-Bath Coupling

The optical excitations of photosynthetic PPCs is well represented by the Frenkel exciton model [39–41]. Correspondingly, we treat a complex of N pigments, each made out of a two-level system representing the Q_y transition in a bacteriochlorophyll (BChl) molecule, interact-

ing through resonance coupling. The Hamiltonian of each individual monomer can be split into the bath, the system and their interaction:

$$H_n = H_B^n + H_S^n + H_{S-B}^n, \quad (1)$$

where

$$H_S^n = (\tilde{\varepsilon}_n + \langle V_e - V_g \rangle) |\tilde{e}_n\rangle\langle \tilde{e}_n| \otimes \mathbb{I}_B^n, \quad (2a)$$

$$H_B^n = (T + V_g) \otimes \mathbb{I}_S^n, \quad (2b)$$

$$\text{and } H_{S-B}^n = (V_e - V_g - \langle V_e - V_g \rangle) \otimes |\tilde{e}_n\rangle\langle \tilde{e}_n|. \quad (2c)$$

Here, V_e (V_g) are the potential energy operators of the bath when the system is in the excited (ground) state, T is the kinetic energy operator of the bath, $\tilde{\varepsilon}_n$ are the site energies of the monomer and $\Delta V = V_e - V_g - \langle V_e - V_g \rangle$ is the so-called energy-gap. $\langle \bullet \rangle$ denotes the equilibrium average over the bath DOF. The ground state energies were taken to be zero for simplicity. The whole complex

is described by the collective ground state $|g\rangle = \Pi_n |g_n\rangle$, one-exciton states $|\bar{e}_n\rangle = \Pi_{a \neq n} |g_a\rangle |\bar{e}_n\rangle$, and higher excited states which we do not consider here. From now on, we stop writing the tensor product \otimes for the sake of brevity. Including the resonance coupling J_{mn} between excited monomers, the total aggregate–bath Hamiltonian reads as

$$H_S + H_B + H_{S-B} = \quad (3)$$

$$\underbrace{\sum_n H_S^n}_{H_0} + \underbrace{\sum_{n \neq m} J_{mn} |\bar{e}_m\rangle \langle \bar{e}_n|}_{H_J} + \sum_n H_B^n + \sum_n H_{S-B}^n.$$

For later use, we split the system Hamiltonian H_S into the part H_0 containing non-interacting pigments and the part H_J containing resonance interaction between the excited states of the pigments. Strong interactions between the pigments (with respect to the pigment–bath interaction) results in a delocalization of the electronically excited states. These can be described as a linear combination of the molecular (local) excited states: $|e_n\rangle = \sum_n c_n^\alpha |\bar{e}_n\rangle$. Such exciton states form the eigenstate basis $\{|e_n\rangle\}$, also known as the excitonic basis, defined such that $H_S |e_n\rangle = \varepsilon_n |e_n\rangle$. When the coupling to the bath is strong compared to the coupling between monomers, the preferred basis is the one formed by the states local to the individual pigments, known as the site basis.

B. Molecular excitons and quantum coherences

The dynamics of electronic energy transfer (EET) processes in molecular aggregates is usually analyzed in a reduced description, where the electronic DOF and their mutual couplings are treated explicitly in the equations of motion, and the electron–environment coupling is integrated into a heat bath representing the environment, and included via some effective quantity, such as the spectral density of the bath. The reduced density matrix (RDM), defined as the trace of the total density matrix over the environmental DOF, $\rho = \text{Tr}_{\text{env}} [|\psi\rangle \langle \psi|]$, provides the maximum information available about the system. If the environment were not present (isolated system), the density matrix would satisfy the Liouville–von Neuman equation with the system Hamiltonian H_S :

$$\frac{\partial}{\partial t} \rho(t) = -\frac{i}{\hbar} [H_S, \rho(t)]. \quad (4)$$

For an open system, the most general equation of motion of the reduced density matrix reads

$$\frac{\partial}{\partial t} \rho(t) = \mathcal{I}(t; \rho(t_0)) - \frac{i}{\hbar} [H_{\text{eff}}, \rho(t)] - \mathcal{D}(t, t_0) \rho(t). \quad (5)$$

The forms of the so-called initial correlation term \mathcal{I} , the effective Hamiltonian H_{eff} and the relaxation tensor

$\mathcal{D}(t, t_0)$ can be derived from the convolutionless projector operator identity [42, 43] and Eq. (5) can be thus regarded formally exact. Despite the fact that the analytical form of the relaxation tensor \mathcal{D} is not known, it is enough for now to notice that the rank four exists. Provided that the system is initially coherently excited, this will drive the system towards the equilibrium and will lead to the decoherence. At long times, the state of the system (in interaction with an equilibrium heat bath) eventually becomes stationary.

For practical reasons, only approximations to the full \mathcal{D} are available to us, although in special cases, exact solutions of various paradigmatic models exist [44]. In some cases, we can find a good approximation to \mathcal{D} by working in an appropriate basis of reduced system’s states. For instance, under weak system–bath coupling, the excitonic basis given by the eigenstate of the system alone is a good starting point of the theory. Ultra fast experiments on photosynthetic antennae can be, to a good degree, described using a relaxation tensor which contains only terms describing population dynamics independent of the off-diagonal elements of the density matrix [45, 46]. The approximation where the influence of the off-diagonal elements of the density matrix on the dynamics of the diagonal elements is neglected is usually termed *secular approximation* [47]. The quality of the secular approximation is obviously dependent on the basis used. If the RDM and its equations of motion, Eq. (5), is transformed into a different basis, e.g. from the excitonic to the site basis, non-secular terms will immediately appear as a consequence of the transformation. The physics however remains the same. The off-diagonal terms of the density matrix are usually termed *coherences* (in plural) and their magnitude is basis dependent. More specifically, the coherence $\rho_{\alpha\beta} = \langle \alpha | \rho | \beta \rangle$ expresses the degree to which a state represented by a given density matrix is a linear combination of the states $|\alpha\rangle$ and $|\beta\rangle$.

Currently, in the field of photosynthesis at least, two distinct phenomena are reported as *coherence* (in singular) in the literature. The first one is related to phase relation between the different pigments, which results from the intermolecular coupling creating non-zero off-diagonal terms in the *site basis* representation – such coherence survives weak coupling of the system to a bath, and demonstrates itself best by stationary coherences (off-diagonal elements of the density matrix) of the equilibrium RDM when represented in the site basis. This phenomenon can be quite directly observed as a splitting or shift of absorption bands of molecular aggregates with respect to the absorption bands of the monomers. The coupling between pigments leads to the formation of delocalized electronic eigenstates in an aggregate. The delocalization of eigenstates is a property intrinsic to the molecular Hamiltonian. The second phenomenon refers to a coherent superposition of excitons (already delocalized excited states), which is a transient time-dependent phenomenon and which is responsible for a coherent wave-like dynamics of EET [7, 8, 10, 12, 14, 48].

Since the coherences related to this phenomenon undergo oscillations in time, they cannot be transformed away by a simple time-independent transformation, and they therefore appear in all bases. In this work, we will refer to *exciton delocalization* and *dynamical coherence* to distinguish between the two effects. The word coherence is thus reserved for the time dependent phenomenon. It is important to note that the exciton delocalization is a well studied and understood phenomenon [40, 46, 49]. It is the dynamical coherence which has recently attracted the attention of the researchers, and we will therefore concentrate solely on the this phenomenon in this paper.

In light of the above discussion on coherence, let us speculate how could dynamical coherence possibly be of use in photosynthetic energy transfer. First of all, if the secular approximation is valid and the coherences are decoupled from the evolution of populations, no amount of coherence could have any influence on the energy transfer dynamics. Non-secular dynamics is therefore required in the first place. It can be shown in the second order perturbation theory that the presence of non-secular terms leads to a correction of the thermal equilibrium. This relates the fact that the equilibrium of an open system subject to a finite coupling to the bath cannot have a canonical form in terms of its own eigenstates. Rather, the whole system of the electronic DOF and the bath would reach equilibrium in a canonical form in terms of the eigenstates of the whole system. The secular approximation usually amounts to approximating the equilibrium of a total system by two separate equilibria – that of the bath and that of the system. Inclusion of the non-secular terms leads to a correction of the stationary long-time state of the system [50]. This state is not diagonal in the basis of the subsystems eigenstates, but the coherence elements of the system are constant. The corresponding RDM could be in principle diagonalized, and the basis in which the system's equilibrium is expressed by a diagonal density matrix could be found. Although the non-secular corrections are usually rather small, in principle they do affect the rate of energy transfer [51]. It is however important to note that this effect occurs whether or not coherences are present, *i.e.* both coherently and incoherently excited systems are driven towards the same equilibrium (canonical or not) on the same time scale. A recent study which clearly distinguishes the different phenomena currently termed quantum coherence in the literature shows that only exciton delocalization can have an effect on energy transfer [52].

Let us, for the sake of an argument, allow for a while that the coherence in the initial state matters, and that the energy transfer between some antennae is more efficient on the level of individual donor-acceptor antenna complex. Then it should be noticed that an ensemble averaging does not influence the enhancement effect. Unlike for coherences, which have a phase and which could be masked by the ensemble averaging, the yield of the energy transfer is additive and it is not masked by the ensemble. This is the case whether the system is ex-

cited by light or by neighboring antenna. As discussed in several works now [35, 36], fully quantum mechanical treatment of the weak light-matter interaction does not lead to time dependent coherences. As demonstrated below, this lack of coherence is caused by integrating over a long time period of the interaction of light and the system. The argument in some papers is that this should be interpreted in terms of individual ultra fast events [33, 53]. If such interpretation is correct and the initial coherence is important for the transfer efficiency, then quantum mechanics is not giving a correct prediction of energy transfer efficiency and the standard prescription for the derivation of measurable outcomes of experiments would have to be replaced by one which takes ultra fast excitation events seriously.

III. INTERACTION OF MOLECULAR AGGREGATES WITH STATIONARY LIGHT

The interaction of molecules with coherent and incoherent light was discussed previously [34–36, 54]. In this section, we extend the results of Ref. [36] to be expressed using experimentally observable quantities. We do not repeat the whole discussion of Ref. [36] which is based on the wavefunction picture and derive the relevant result using the density matrix formalism. Nevertheless, the point of the derivation is that the dynamics of the quantum system occurs as a continuous change of the system's state, which should not be interpreted as representing actual discontinuous quantum jumps. Below, we present the interaction of an aggregate of coupled molecules with light in an arbitrary state and, if the state is stationary, we show how the system density matrix evolution can be expressed by means of the spectrum of the incident radiation and the absorption spectrum of the system.

A. System Interaction with Weak Light

Let us consider our aggregate interacting with light. The total Hamiltonian is

$$H = H_S + H_B + H_{S-B} + H_L + H_{S-L}, \quad (6)$$

where $H_L = \sum_{q,\lambda} \hbar\omega_q a_{q\lambda}^\dagger a_{q\lambda}$ is the Hamiltonian of light and $H_{S-L} = -\mu \cdot E(t)$ is the interaction of the system with light in dipole approximation. We neglect the interaction of light with the bath. The dipole moment operator in exciton basis reads $\mu = \sum_i \mu_{ig} |e_i\rangle \langle g| + h.c.$ and the electrical field in second quantization is $\mathbf{E}(t) = i \sum_{q,\lambda} \sqrt{\frac{\hbar\omega_q}{2\epsilon_0 V}} e_{q,\lambda} \left(a_{q\lambda} e^{-i\omega_q t} - a_{q\lambda}^\dagger e^{i\omega_q t} \right)$. For the sake of simplicity, we omit the light polarization from now on.

The time evolution of the density matrix is given by Liouville-von Neuman equation using the Hamiltonian detailed in Eq. (6). Treating the interaction with light as a perturbation, expanding into second order and rewrit-

ing everything in terms of the Liouville space superoperators (see e.g. [55]), we obtain

$$\rho^{(2)}(t) = \int_{t_0}^t d\tau \int_{t_0}^{\tau} d\tau' \mathcal{U}(t-\tau) \mathcal{V}(\tau) \mathcal{U}(\tau-\tau') \mathcal{V}(\tau') \rho(t_0). \quad (7)$$

Here $\mathcal{U}(t) \bullet = U(t) \bullet U^\dagger(t)$ is a Liouville space propagator and $\mathcal{V}(t) \bullet = \frac{1}{\hbar} [\mu, \bullet] \cdot E(t)$ is the interaction with light. The initial density matrix is taken as the factorized, unentangled form

$$\rho(t_0) = |\Xi_0\rangle|g\rangle\langle g| \langle \Xi_0| \otimes \rho_{eq}^B, \quad (8)$$

which consists of the system in ground state $|g\rangle$, the light in an initial state $|\Xi_0\rangle$ and the bath in equilibrium. Because we are interested in the dynamics of the system, we pass into the reduced description, tracing over the light and bath degrees of freedom, and

$$\rho_S^{(2)}(t) = \text{Tr}_{B,L} \int_{t_0}^t d\tau \int_{t_0}^{\tau} d\tau' \mathcal{U}(t-\tau) \mathcal{V}(\tau) \mathcal{U}(\tau-\tau') \mathcal{V}(\tau') \rho(t_0). \quad (9)$$

Following the detailed description in Ref. [36], we rewrite this expression into the form

$$\begin{aligned} \rho_S^{(2)}(t) &= \frac{1}{\hbar^2} \int_{t_0}^t d\tau \int_{t_0}^{\tau} d\tau' \langle \Xi_0 | E^{(-)}(\tau) E^{(+)}(\tau') | \Xi_0 \rangle \\ &\times \text{Tr}_B \{ \mathcal{U}_0(t-\tau) [\mu, \mathcal{U}_0(\tau-\tau') [\mu, |g\rangle\langle g|]] \otimes \rho_{eq}^B \}. \end{aligned} \quad (10)$$

Here, $E^{(-)}(t)$ is the negative frequency part of $E(t)$, including a^\dagger , $E^{(+)}(t)$ is its Hermitian conjugate, and $\mathcal{U}_0(t)$ is the propagator with $H_S + H_B + H_{S-B}$. This expression corresponds to Eq. (70) in [36]. We can see that the first term under the integration is the correlation function of the light, and that the second term corresponds to a light-induced dynamics of the system in contact with a bath.

B. Thermal Light Description

Because our main goal is to describe the interaction of the aggregate with sunlight and to see if it is any different from the interaction with for instance the laser field, we present here a short derivation of the thermal light correlation function. The thermal light density matrix can be written as [56]

$$\rho_L = \prod_{\otimes k, \lambda} \sum_{n_{k\lambda}} \frac{\langle n_k \rangle^{n_{k\lambda}}}{(1 + \langle n_k \rangle)^{1+n_{k\lambda}}} | \{ n_{k\lambda} \} \rangle \langle \{ n_{k\lambda} \} | \quad (11)$$

where $| \{ n_{k\lambda} \} \rangle$ forms the basis of photon number states in mode k and with polarization λ and $\langle n_k \rangle$ is the average number of photons in the corresponding mode.

The first-order correlation function is then

$$\begin{aligned} \langle E^{(-)}(\tau) E^{(+)}(\tau') \rangle &= \sum_{q\lambda, q'\lambda'} \frac{\hbar \sqrt{\omega_q \omega_{q'}}}{2\varepsilon_0 V} e^{i\omega_q \tau - i\omega_{q'} \tau'} \\ &\times \text{Tr} \{ a_{q\lambda}^\dagger a_{q'\lambda'} \rho_L \} \\ &= 2 \sum_k \frac{\hbar \omega_k}{2\varepsilon_0 V} e^{i\omega_k(\tau-\tau')} \langle n_k \rangle. \end{aligned} \quad (12)$$

Considering a Bose-Einstein distribution of the mode populations $\langle n_k \rangle = 1/(e^{\hbar\omega_k/k_B T} - 1)$ and passing from mode summation to frequency integration, we obtain

$$\langle E^{(-)}(\tau) E^{(+)}(\tau') \rangle = \int_0^\infty d\omega \frac{\hbar}{\varepsilon_0 2\pi^2 c^3} \frac{\omega^3}{e^{\hbar\omega/k_B T} - 1} e^{i\omega(\tau-\tau')}, \quad (13)$$

where the integrated expression without the exponential is a Planck's law. Thus, the first-order correlation function for thermal light is stationary, *i.e.* is a function of the difference $(\tau - \tau')$, and can be expressed as a Fourier transform of the spectrum $W(\omega)$ of the light:

$$\mathcal{G}^{(1)}(\tau) = \langle E^{(-)}(\tau) E^{(+)}(0) \rangle = \int_0^\infty d\omega W(\omega) e^{i\omega\tau}. \quad (14)$$

More generally, this formula holds for stationary light and is known as the Wiener-Khinchine theorem [56].

C. Aggregate in Stationary Light

Let us now insert the general expression corresponding to a stationary correlation function, Eq. (14), into the second-order density matrix expansion, Eq. (10):

$$\begin{aligned} \rho_S^{(2)}(t) &= \frac{1}{\hbar^2} \int_0^\infty d\omega W(\omega) \int_{t_0}^t d\tau \int_{t_0}^{\tau} d\tau' e^{i\omega(\tau-\tau')} \\ &\times \text{Tr}_B \{ \mathcal{U}_0(t-\tau) [\mu, \mathcal{U}_0(\tau-\tau') [\mu, |g\rangle\langle g|]] \otimes \rho_{eq}^B \}. \end{aligned} \quad (15)$$

We now have a general description of the aggregate weakly coupled to the bath interacting with stationary light. For our purpose, we will treat the system-bath interaction by means of cumulant expansion [55]. The propagators are then expressed by means of the optical transition frequencies ω_{ig} , population relaxation rates Γ and the line shape function $g(t)$. The a -th population element of the density matrix $P_a(t) = \langle a | \rho_S^{(2)}(t) | a \rangle$ is then

$$\begin{aligned} P_a(t) &= \frac{1}{\hbar^2} |\mu_{ag}|^2 2 \text{Re} \int_0^\infty d\omega W(\omega) \\ &\times \int_{t_0}^t d\tau \int_{t_0}^{\tau} d\tau' e^{i\omega(\tau-\tau')} e^{-\Gamma(t-\tau)} e^{-g(\tau-\tau') - i\omega_{ag}(\tau-\tau')}, \end{aligned} \quad (16)$$

where Re denotes the real part. By substitution of $(\tau - \tau')$, we obtain:

$$\begin{aligned} P_a(t) &= \frac{|\mu_{ag}|^2}{\hbar^2} 2 \text{Re} \int_0^\infty d\omega W(\omega) \\ &\times \int_{t_0}^t d\tau e^{-\Gamma(t-\tau)} \int_0^{\tau-t_0} d\tau' e^{i\omega\tau'} e^{-g(\tau') - i\omega_{ag}\tau'}. \end{aligned} \quad (17)$$

Because the line shape function gives dephasing of the optical coherences with characteristic time ~ 10 -100 fs, we can formally send $t_0 \rightarrow -\infty$. The τ' integral then yields the absorption spectrum of the a -th exciton defined as

$$\chi_a(\omega) = |\mu_{ag}|^2 2 \operatorname{Re} \int_0^\infty d\tau' e^{i\omega\tau'} e^{-g(\tau') - i\omega_{ag}\tau'}. \quad (18)$$

We can now perform the τ integration and obtain

$$P_a(t) = \frac{1}{\hbar^2} \int_0^\infty d\omega W(\omega) \chi_a(\omega) \frac{1 - e^{-\Gamma(t-t_0)}}{\Gamma}. \quad (19)$$

For relatively long evolution times ($t - t_0$) compared to the population dephasing time, we can neglect the exponential. This results in constant population of the a -th exciton:

$$P_a(t) = \frac{1}{\hbar^2} \frac{1}{\Gamma} \int_0^\infty d\omega W(\omega) \chi_a(\omega), \quad (20)$$

as in [34]. For short (but still longer than coherence dephasing) times ($t - t_0$), we can expand the exponential and thus get a transient linear growth of the population

$$P_a(t) = \frac{1}{\hbar^2} (t - t_0) \int_0^\infty d\omega W(\omega) \chi_a(\omega), \quad (21)$$

as in [36]. In both cases, the population depends on the overlap of the spectrum of the incident light with the absorption spectrum of the given exciton. We emphasize that the only properties of light which play a role here are its stationarity and the integrated overlap of its spectrum with the absorption spectrum of the aggregate. Therefore, the light-induced population kinetics will essentially be the same under excitation by sunlight and for instance laser light, with possible differences arising only in the absolute value of the final population and the absorption rate.

Another question is to quantify the coherences, *i.e.* superpositions of excitons. A calculation similar to that presented above gives the off-diagonal elements of the system density matrix as:

$$P_{ab}(t) = \frac{1}{\hbar^2} \int_0^\infty d\omega W(\omega) \left[\frac{\mu_{gb}}{\mu_{ga}} \tilde{\chi}_a(\omega) + \frac{\mu_{ag}}{\mu_{bg}} \tilde{\chi}_b^*(\omega) \right] \frac{1}{i\omega_{ab} + \Gamma} \quad (22)$$

where $\tilde{\chi}_a(\omega) = \int_0^\infty d\tau e^{i\omega\tau} e^{-i\omega_{ag}\tau - g(\tau)}$ is the complex susceptibility of the a -th exciton. Notice that the coherences are stationary. Also, for non-relaxing populations, the fraction goes to a delta function $\delta(\omega_{ab})$, which means that the coherences tend to zero and the density matrix is diagonal, *i.e.* the state becomes a statistical mixture of populated states. The expression for populations then corresponds to Eq. (20). When a particular model for the line shape functions is introduced, explicit results for populations and coherences values can be obtained in agreement with Ref. [36].

IV. FÖRSTER TYPE ENERGY TRANSFER: WAVEFUNCTION PERSPECTIVE

Let us now turn our attention to the excitation of an antenna system by a neighboring antenna. This situation will be modeled here by an energy transfer between two excited states $|1\rangle$ and $|2\rangle$ of a simple donor-acceptor system. The two states correspond to the site basis collective states of the aggregate:

$$|1\rangle = |\tilde{e}_1\rangle|g_2\rangle, \quad |2\rangle = |g_1\rangle|\tilde{e}_2\rangle. \quad (23)$$

Let us assume the initial condition for the energy transfer to correspond to the usual assumptions behind the derivation of the Förster energy transfer rates, *i.e.* the donor is in the excited state with the bath relaxed to the equilibrium corresponding to the excited state potential energy surface, while the acceptor is in the ground state with the bath relaxed to the equilibrium corresponding to the ground state potential energy surface. Here, we assume that the molecule 1 is the donor with the probability $\rho_{11} \equiv |c_1|^2$ and the molecule 2 is the donor with the probability $\rho_{22} \equiv |c_2|^2$ (both molecules are partly donors and acceptors). The quantum mechanical state of the electronic system can be expressed as usual by a reduced density matrix

$$\rho(t_0) = \sum_n \rho_{nn} |n\rangle\langle n|. \quad (24)$$

Such a reduced density matrix can be obtained from tracing of a density operator corresponding to the compound system of the donor-acceptor dimer and its environment, which has a form

$$W_0 \equiv |\Psi_0\rangle\langle\Psi_0|, \quad (25)$$

where

$$|\Psi_0\rangle \equiv |\Psi(t_0)\rangle = c_1|1\rangle|\psi_1\rangle + c_2|2\rangle|\psi_2\rangle. \quad (26)$$

The bath wavefunctions $|\psi_n\rangle$ copy the structure of the excitonic state, Eq. (23), and can be written as:

$$|\psi_1\rangle = |\psi_1^{(e)}\rangle|\psi_2^{(g)}\rangle, \quad (27a)$$

$$|\psi_2\rangle = |\psi_1^{(g)}\rangle|\psi_2^{(e)}\rangle. \quad (27b)$$

Here, the state $|\psi_1^{(e)}\rangle$ is the state of the environment of pigment 1 relative to its excited state, and analogically for the other states in Eq. (27). We require the overlap of the bath wavefunctions to be zero:

$$\langle\psi_1|\psi_2\rangle = 0. \quad (28)$$

To the second order in the resonance coupling Hamiltonian H_J (see Eq. (3)), the total wavefunction of the system reads

$$\begin{aligned} |\Psi(t)\rangle &= U(t)|\Psi_0\rangle - \frac{i}{\hbar} \int_{t_0}^t d\tau U(t-\tau) H_J U(\tau) |\Psi_0\rangle \\ &\quad - \frac{1}{\hbar^2} \int_{t_0}^t d\tau \int_{t_0}^{\tau} d\tau' U(t-\tau) H_J U(\tau-\tau') H_J U(\tau') |\Psi_0\rangle. \end{aligned} \quad (29)$$

Here, $U(t) = \exp\{-\frac{i}{\hbar}H_0t\}$ is the evolution operator of the non-interacting pigments. The population probab-

ility of the electronic state $|1\rangle$ now reads, to the second order:

$$\begin{aligned} \rho_{11}(t) = \langle \Psi(t)|1\rangle\langle 1|\Psi(t)\rangle &= \rho_{11}(t_0) - \frac{2}{\hbar} \text{Im} \left\{ \int_{t_0}^t d\tau \langle \Psi_0|1\rangle\langle 1|U^\dagger(\tau)H_JU(\tau)|\Psi_0\rangle \right\} \\ &- \frac{2}{\hbar^2} \text{Re} \left\{ \int_{t_0}^t d\tau \int_{t_0}^\tau d\tau' \langle \Psi_0|1\rangle\langle 1|U^\dagger(\tau)H_JU(\tau-\tau')H_JU(\tau')|\Psi_0\rangle \right\} \\ &+ \frac{1}{\hbar^2} \int_{t_0}^t d\tau \int_{t_0}^\tau d\tau' \langle \Psi_0|U^\dagger(\tau)H_JU^\dagger(t-\tau)|1\rangle\langle 1|U(t-\tau')H_JU(\tau')|\Psi_0\rangle. \end{aligned} \quad (30)$$

The first order (in H_J) integral term of Eq. (30) is zero due to the assumption of Eq. (28). indeed, we can write

$$\begin{aligned} \langle \Psi_0|1\rangle\langle 1|U^\dagger(\tau)H_JU(\tau)|\Psi_0\rangle &= c_1c_2J_{12}\langle \psi_1|U_1^\dagger(\tau)U_2(\tau)|\psi_2\rangle \\ &= c_1c_2J_{12}\langle \psi_1|\psi_2\rangle \\ &= 0, \end{aligned} \quad (31)$$

where the omission of the evolution operators is allowed

because the evolution of the state which is in equilibrium does not bring any changes to the value of the wavefunction overlap. The last term in Eq. (30) can be split into the one where $\tau > \tau'$ and the one where $\tau < \tau'$. We find that these two terms are mutually complex conjugate, and therefore write

$$\begin{aligned} \rho_{11}(t) &= \rho_{11}(t_0) - \frac{2|J_{12}|^2}{\hbar^2} \text{Re} \left\{ \int_{t_0}^t d\tau \int_{t_0}^\tau d\tau' \langle \psi_1|U_1^\dagger(\tau)U_2(\tau-\tau')U_1(\tau')|\psi_1\rangle \right\} |c_1|^2 \\ &+ \frac{2|J_{12}|^2}{\hbar^2} \text{Re} \left\{ \int_{t_0}^t d\tau \int_{t_0}^\tau d\tau' \langle \psi_2|U_2^\dagger(\tau)U_1(\tau-\tau')U_2(\tau')|\psi_2\rangle \right\} |c_2|^2. \end{aligned} \quad (32)$$

Because the bath states $|\psi_1\rangle$ and $|\psi_2\rangle$ represent the bath equilibria with respect to given electronic states, their propagation in time governed by the evolution operator corresponding to the potential energy surface of that electronic state does not change the value of the matrix elements under integration in Eq. (32). We therefore have, e.g.

$$\begin{aligned} &\langle \psi_2|U_2^\dagger(\tau)U_1(\tau-\tau')U_2(\tau')|\psi_2\rangle \\ &= \langle \psi_2|U_2^\dagger(\tau-\tau')U_1(\tau-\tau')|\psi_2\rangle. \end{aligned} \quad (33)$$

Taking a time derivative of Eq. (32) and performing a substitution $(t-\tau) \rightarrow \tau$, we obtain

$$\frac{\partial}{\partial t}\rho_{11}(t) = -K_{11}(t-t_0)\rho_{11}(t_0) + K_{12}(t-t_0)\rho_{22}(t_0), \quad (34)$$

where

$$K_{11}(t-t_0) = \frac{2|J_{12}|^2}{\hbar^2} \text{Re} \left\{ \int_0^{t-t_0} d\tau \langle \psi_1|U_1^\dagger(\tau)U_2(\tau)|\psi_1\rangle \right\}, \quad (35)$$

and

$$K_{12}(t-t_0) = \frac{2|J_{12}|^2}{\hbar^2} \text{Re} \left\{ \int_0^{t-t_0} d\tau \langle \psi_2|U_2^\dagger(\tau)U_1(\tau)|\psi_2\rangle \right\}, \quad (36)$$

correspond to the depopulation rate of the state $|1\rangle$ and the rate of population transfer from state $|2\rangle$ to state $|1\rangle$, respectively. The matrix elements under the integration are expressed in terms of collective states. When expressed in the quantities corresponding to individual

pigments, we arrive at the following

$$\begin{aligned}
& \langle \psi_2 | U_2^\dagger(\tau) U_1(\tau) | \psi_2 \rangle \\
&= \langle \psi_2^{(e)} | \langle \psi_1^{(g)} | U_2^{(e)\dagger}(\tau) U_1^{(g)\dagger}(\tau) U_1^{(e)}(\tau) U_2^{(g)}(\tau) | \psi_1^{(g)} \rangle | \psi_2^{(2)} \rangle \\
&= \langle \psi_1^{(g)} | U_1^{(g)\dagger}(\tau) U_1^{(e)}(\tau) | \psi_1^{(g)} \rangle \langle \psi_2^{(e)} | U_2^{(e)\dagger}(\tau) U_2^{(g)}(\tau) | \psi_2^{(2)} \rangle \\
&= e^{-g_{11}(\tau)} e^{-g_{22}^*(\tau) - 2i\lambda\tau},
\end{aligned} \tag{37}$$

where in the last step we have used the second cumulant expansion (see Ref. [55]) to obtain the matrix elements in terms of the line shape functions $g_{11}(t)$ and $g_{22}(t)$ of the pigment 1 and 2, respectively. Not surprisingly, the rates are time dependent.

The final expression can be obtained by assuming $t - t_0$ large, *i.e.* formally $t - t_0 \rightarrow \infty$. This yields

$$K_{11} = \frac{2|J_{12}|^2}{\hbar^2} \text{Re} \left\{ \int_0^\infty d\tau e^{-g_{11}^*(\tau) - 2i\lambda_{11}\tau - g_{22}(\tau)} \right\}, \tag{38}$$

and

$$K_{12} = \frac{2|J_{12}|^2}{\hbar^2} \text{Re} \left\{ \int_0^\infty d\tau e^{-g_{11}(\tau) - g_{22}^*(\tau) - 2i\lambda_{22}\tau} \right\}. \tag{39}$$

These expressions correspond to the well-known Förster rates.

We can now return back to the expression of wavefunction, Eq. (29), from which we derived the Förster rates. Inserting Eq. (26) into Eq. (29) we obtain

$$\begin{aligned}
|\Psi(t)\rangle &= \left(c_1 |\psi_1\rangle - c_2 \frac{iJ_{12}}{\hbar} (t - t_0) |\psi_{1\leftarrow 2}(t)\rangle - c_1 \frac{|J_{12}|^2}{\hbar^2} (t - t_0)^2 |\psi_{1\leftarrow 2\leftarrow 1}(t)\rangle \right) |1\rangle \\
&+ \left(c_2 |\psi_2\rangle - c_1 \frac{iJ_{12}}{\hbar} (t - t_0) |\psi_{2\leftarrow 1}(t)\rangle - c_2 \frac{|J_{12}|^2}{\hbar^2} (t - t_0)^2 |\psi_{2\leftarrow 1\leftarrow 2}(t)\rangle \right) |2\rangle.
\end{aligned} \tag{40}$$

Here, we defined the bath wavefunctions

$$|\psi_{m\leftarrow n}(t)\rangle = \frac{1}{t - t_0} \int_{t_0}^t d\tau U_m(t - \tau) U_n(\tau) |\psi_n\rangle, \tag{41}$$

$$\begin{aligned}
|\psi_{m\leftarrow n\leftarrow m}(t)\rangle &= \\
&\frac{1}{(t - t_0)^2} \int_{t_0}^t d\tau \int_{t_0}^\tau d\tau' U_m(t - \tau) U_n(\tau - \tau') U_m(\tau') |\psi_m\rangle.
\end{aligned} \tag{42}$$

In principle, Eq. (29) or (40) can be used iteratively to obtain a full time evolution of the system.

It is important to note that during such a propagation, the dynamics obtained in terms of populations corresponds to the one usually termed incoherent or classical hopping. Nevertheless, in the dynamics itself, there is no trace of actual hopping, and from the point of view of the system's wavefunction, the evolution is entirely continuous. The need for discontinuous jumps, which is so often expressed through the postulation of sharp initial conditions seem to only stem from certain interpretation of the quantum mechanics in which macroscopically (and therefore classically) observable states are prescribed from outside the quantum mechanics, and in which the system described by an incoherent density matrix is required to *be* in one of the classical states. The emergence of this classicality from quantum mechanics can be, however, explained from within the quantum theory [57–59], and

Eq. (40) demonstrates that an individual molecular system can *be* in a state which corresponds to an incoherent density matrix with a continuous change of population probabilities.

V. EXCITATION DYNAMICS UNDER VARIOUS EXCITATION CONDITIONS

Now that we have argued that an excitation transfer from one to another antenna by an incoherent rate process cannot be interpreted in a statistical way as a series of individual jumps of some ultra fast duration, we can study how such process can lead to a creation of coherence in the acceptor antenna. We will take the most favorable situation for creation of acceptor coherence, *i.e.* a situation that the excitation has arrived in an ultra fast fashion at the donor, and it proceeds from there to the acceptor with certain rate. For comparison, we study several different excitation conditions, and we also compare with the dynamics of a dissipation (and therefore decoherence) free system.

As a model system, we will take the chlorosome-FMO complex of the *Chlorobium tepidum* bacteria, with the chlorosome simplified into a single pigment of its baseplate. We will postulate a simple variant of Eq. (5) with constant rate coefficients for the internal energy relaxation inside the FMO and a single transfer rate (possibly of the Förster type) from the chlorosome to the FMO.

The FMO complex of green sulfur bacteria is the first photosynthetic PPC for which the structure was determined by X-ray crystallography [60] and has been extensively studied since then [61]. It is a homotrimer consisting of bacteriochlorophyll-a (BChl-a) molecules that transfer excitation energy between the baseplate protein of the chlorosome and the reaction center (RC). Since the strongest electronic coupling between BChls of different monomer subunits is about one order of magnitude weaker than the local reorganization energies [62], we assume each monomer to function independently and accordingly study the EET dynamics within one single subunit. Most of the studies describe each monomer as a set of seven BChls, but recent crystallographic studies reported the existence of an eighth BChl molecule [63, 64]. We present detailed calculation using the *apo* form (seven BChls per monomer) of the FMO protein (system Hamiltonian from Ref. [62]). Results using the *holo* form (eight BChls per monomer, Hamiltonian from Ref. [65]) present a similar dynamics and are therefore not presented here. Based on theoretical calculations [62] and recent experimental verification [66], the FMO complex is assumed to be oriented with BChls 1 and 6 toward the baseplate protein, whereas BChls 3 and 4 are at the interface between the FMO and the reaction center. Accordingly, the initial excited pigments in our numerical calculations are chosen to be either BChls 1 or 6.

Despite the fact that we have chosen a very particular model system, the particularities of the model are not the focus of the interest here. Rather, we want to demonstrate some of the statements from Section II B and to show that even a system where coherences are not damped by dissipative dynamics cannot be coherently excited by energy transfer from neighboring antenna. In order for our analysis to be quantitative, we define a measure of the excitonic coherence Ξ such as:

$$\Xi = \frac{\sum_{\alpha,\beta} \xi(\rho) \cdot (\rho_{\alpha\alpha} + \rho_{\beta\beta})}{(N-1) \sum_1^N \rho_{\alpha\alpha}}, \quad (43)$$

where $\xi(\rho) = \frac{|\rho_{\alpha\beta}|^2}{\rho_{\alpha\alpha}\rho_{\beta\beta}}$ defines the excitonic coherences between the two excited states α and β ($\xi = 1$ for a completely coherent system), and is weighted by the population probabilities of the corresponding states to only account for the significantly populated coherent states. It is easy to verify that $\Xi = 1$ for a purely coherent system, and $\Xi = 0$ when no superposition is present. Note that the amount of coherence is a time-dependent variable when the system of interest is subjected to relaxation due to some interaction with bath DOF. It also is a basis dependent quantity in line with the basis dependent properties of the coherences.

A. Ultra Fast Single-Site Excitation

Let us start with studying an ultra fast excitation of a single site of the complex. This is an often applied but

rather artificial initial condition, as it cannot be created by light, both due to spatial (wavelength) and spectral reasons. It is important to realize that in a coupled complex, single site represents a linear combination of the eigenstates of the complex, and therefore its excitation induces coherent dynamics.

Figure 1 presents the EET dynamics in both the site and excitonic basis after an ultra fast excitation of BChl 1 (A) or BChl 6 (B), with or without relaxation. As expected from the aggregate conformation, more specifically from the excitonic heterodimer formed by BChls 1 and 2, an excitation initially located on BChl 1 is transferred and shared with BChl 2 (see the site basis representation, Figs. 1A1 and 1A3). Populations display an out-of-phase evolution at the frequency $\omega_{12} = (E_1 - E_2)/\hbar$, which corresponds to the frequency of the coherence evolution. In the eigenstate basis, Figs. 1A2 and 1A4, the excitation of BChl 1 populates exciton levels 3 and 6 (excitons are ordered with increasing eigenenergies), which is in concordance with previous studies (see e.g. [62]). Without interactions with the bath, it is verified that this initial condition leads to a pure state (*i.e.* $|\rho_{36}| = \sqrt{\rho_{33}\rho_{66}}$) with long-lived dynamical coherences developing between the two excitons oscillating at the frequency $\omega_{36} = (\varepsilon_3 - \varepsilon_6)/\hbar$. In this (eigenstate) basis, it is seen that the exciton populations are constant, and that only coherences evolve phase. Comparison of the results presented in the site and excitonic basis (top *vs* bottom) illustrates that dynamical oscillations of the RDM off-diagonal terms, though basis dependent, are observed in both basis. When considering a Markovian dynamics in secular approximation, beating can still be observed on the real part of the off-diagonal terms. However, due to the interactions with the bath, the oscillations are damped in ~ 700 fs.

Figure 1B presents results when the excitation is initially received by BChl 6. The relaxation pathway now involves BChls 5 and 6 and, to a smaller extent, BChl 7 (see Figs. 1B1 and 1B3). Excitons 7 and 5 are the main contributors to this transfer branch (Figs. 1B2 and 1B4). Similarly to the previous case, an oscillatory behavior can be observed here, also in both basis. Beating develops between sites 5 and 6 (site basis) and between excitons 5 and 7 (excitonic basis). In the ideal assumption of a free exciton system, long-lived oscillations are observed in both basis. When considering coupling with the bath DOF, these oscillations are quickly damped (in ~ 400 fs).

Note that the off-diagonal terms of the RDM, in the local basis, stabilize around a non-zero value, but that in the basis relevant to the observation of dynamical coherences (excitonic basis), those terms quickly equal zero. This difference originates from the two distinct phenomena presented in Section II B. In the local basis, the non-zero values indicate delocalization of the exciton, whereas in the excitonic basis representation, no long-lived dynamical coherence survive when the system is interacting with its environment (although the bath DOF are

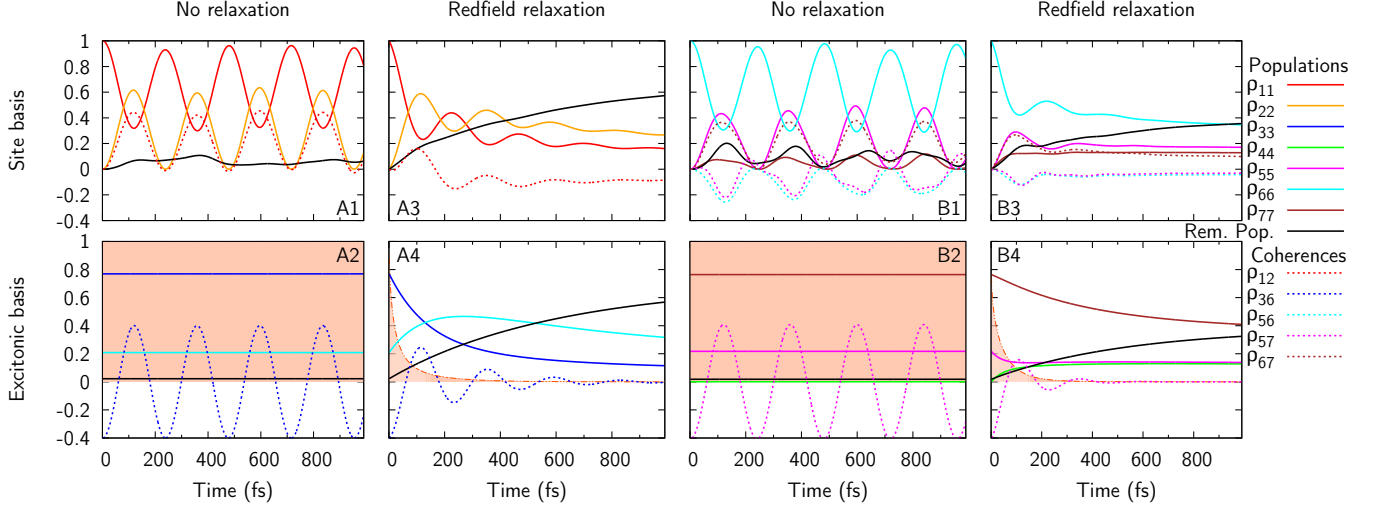


Figure 1: Time evolution of populations and coherences (diagonal and off-diagonal terms of the RDM, respectively) in the site (top) and excitonic basis (bottom) after excitation of BChl 1 (A) or 6 (B) in a free exciton system (1;2) or with Redfield form of relaxation (3;4). The shaded area represents the amount of coherence in the system (Eq. 43).

assumed to be totally correlated).

The amount of coherence Ξ (as defined in Eq. 43) is highlighted with a shaded area to illustrate the amount of dynamical coherence in the system. As mentioned above, this quantity is only relevant in the excitonic basis. In a free exciton system, an initially coherent system remains purely coherent and accordingly $\Xi = 1$. However, the amount of coherence is damped when the system interacts with the bath DOF, and it is verified that $\Xi(t)$ follows a decay similar to the dynamical coherences.

B. Ultra Fast Multi-Site (Laser) Excitation

To go beyond the single site excitation, we present results of EET dynamic in an initially purely coherent system assuming all sites to be excited with equal probabilities after interaction with an ultra short laser pulse (in reality, one should account for the averaged direction of the BChls' transition dipole moment relatively to the laser pulse, but this simplification does not limit the discussion presented below). Fig. 2A1 shows that, in a free exciton system, the populations and coherences evolve phase at their own rate in the site basis, while in the excitonic basis (Fig. 2A2), the exciton populations remain constant and the dynamical coherence between eigenstate α and β oscillate at a frequency $\omega_{\alpha\beta} = (\varepsilon_{\alpha} - \varepsilon_{\beta})/\hbar$. When considering relaxation to the bath, the amount of coherence present in the system is quickly damped (~ 500 fs), as seen from $\Xi(t)$ in the excitonic basis representation. Here also, the value of the coherence terms quickly reaches zero in the excitonic basis, whereas they stabilize at a non-zero value in the site basis because of the coupling between the site and resulting delocalization of excitons.

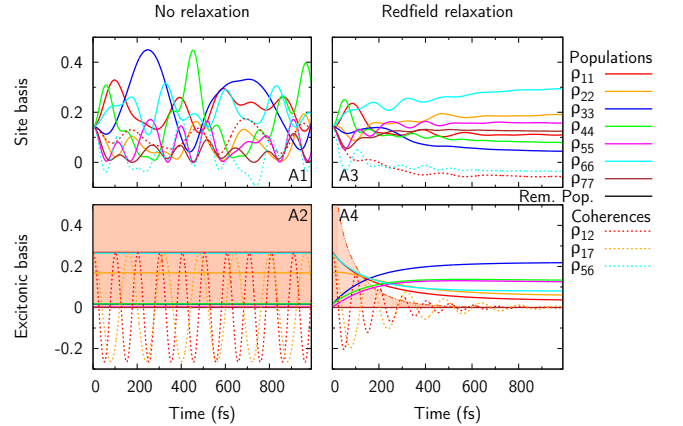


Figure 2: Time evolution of the populations and coherences in the site (top) and excitonic basis (bottom) of a purely coherent system at initial time (laser excitation), without (1;2) and with Redfield (3;4) relaxation. The shaded area represents the amount of coherence in the system (Eq. 43).

These results display a behavior similar to that observed after excitation of one single site, confirming that excitation by a laser pulse – which will excite various BChls according to the orientation of their transition dipole moment – can be used to study EET in a FMO complex although such condition does not correspond to the natural excitation, *i.e.* feeding of BChls 1 and 6 from the baseplate protein. However, one should keep in mind that the beating is not only basis dependent, but also depends on the initial excitation conditions, as can be seen from the differences arising between Figs. 1 and 2 (same oscillatory behavior, but with different coherence amplitude, frequency and life time).

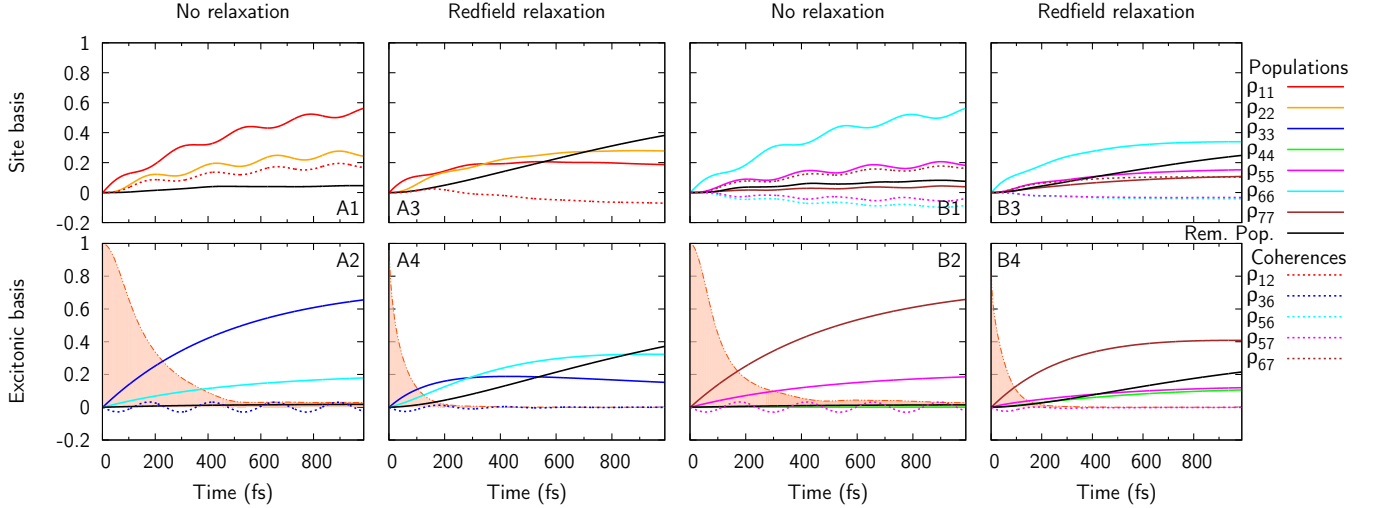


Figure 3: Time evolution of populations and coherences in the site (top) and excitonic basis (bottom) when BChl 1 (A) or 6 (B) is excited with a feeding rate of 500 fs^{-1} in a free exciton system (1;2) or assuming a Redfield form of relaxation (3;4). The shaded area, which represents the amount of coherence in the system, shows that even without any relaxation dynamical coherences die out because of destructive interferences.

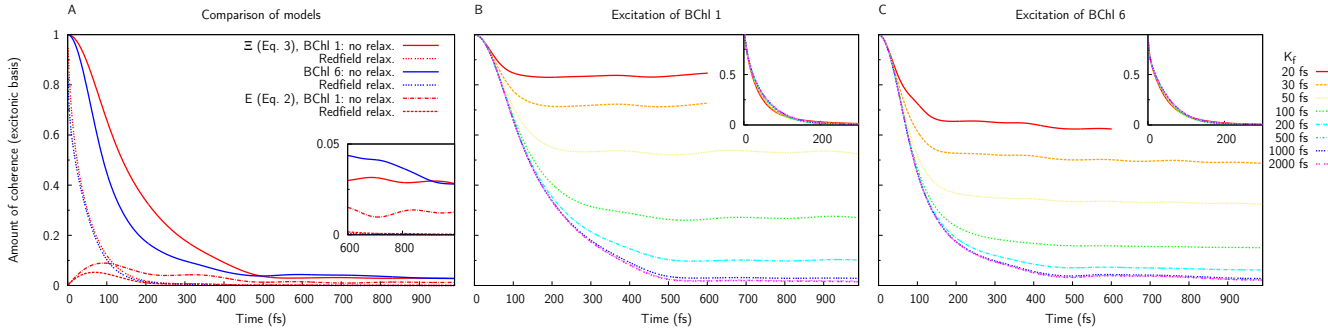


Figure 4: Evolution of the amount of coherence. (A) Comparison of the models defined in Eq. 43 and Ref. [67] with an excitation rate of 500 fs^{-1} (the inset shows a detail of the results at long time). (B and C) Amount of coherence for different excitation rates of BChl 1 and BChl 6, respectively in a free exciton system. The insets show results using a Redfield type of relaxation. It is shown that excitation from neighboring antennae (feeding rate of tens of picoseconds) can not lead to a coherent superposition of excited states.

C. Excitation by Neighboring Antennae

Now we finally consider the response of an aggregate when surrounded by its neighboring antennae. The complex starts in its ground state, and the excitation is introduced from the source s (representing the neighboring BChls of the chlorosomal baseplate) to the system via BChl i at a feeding rate K_f such as:

$$\frac{\partial \rho_{ii}(t)}{\partial t} = K_f \rho_{ss}(t). \quad (44)$$

Fig. 3 shows the corresponding dynamics of EET when BChl 1 or 6 are excited at a rate of 500 fs^{-1} . Results show that the growing population of BChl 1 is slowly populating BChl 2 (see Figs. 3A1 and 3A3), which is equivalent, in the excitonic basis, of populating excitons 3 and 6 (see

Figs. 3A2 and 3A4). However, even without any relaxation, this transfer does not generate a large superposition of states, as indicated from the small amplitude of the coherence oscillations observed in the excitonic basis (see Fig. 3A2). Contrary to the case where a single excitation of BChl 1 leads to a coherent dynamics (Fig. 1A2), the amount of coherence here quickly decreases with increasing populations, and it is very low when the system is significantly populated ($\Xi < 0.04$ after 500 fs^{-1}). This can be explained by interferences building up between coherences of excited states created at different times (which correspond to different phases) according to the feeding rate, such that: $\rho_{\alpha\beta}(t) \propto \int_0^t d\tau e^{i\omega_{\alpha\beta}/\hbar t} e^{i\phi(\tau)}$. Upon continuous feeding of BChl 1 from the neighboring antenna, the integration over different phases $\phi(\tau)$ will result in destructive interferences, which are created within a *single* complex and prevent any dynamical co-

herent superposition of excited states.

Figures 3Bs show the results when excitation from the neighboring antennae is received by BChl 6. Such a configuration results in a similar dynamics through the population of mainly BChl 5 and 6 and excitons 7 and 5. The evolution of the amount of coherence is alike to the former case, without any creation of eigenstate superposition. Relaxation through interaction with the bath DOF will certainly not help to maintain coherent transfer, and in this case, the dynamical coherences are damped even faster – $\Xi(500\text{fs}^{-1}) < 0.01$ in both excitation conditions – as shown by Figs. 3A4 and 3B4.

In Figure 4A, we present the amount of coherence calculated according to Eq. 43 and comparison with the model defined in Ref. [67]. It appears that although the different models provide very different amount of coherence in the system at initial time (very low populations), after a transient effect and once the population of the excited site becomes significant ($\sim 500 \text{ fs}^{-1}$ here), both models clearly show that no dynamical coherence survive, independently of the site excitation and dissipation to the bath.

Using Eq. 43 to compute the amount of coherence Ξ in the system, we present the results for different excitation conditions (site 1 or 6 with various feeding rates) in a free exciton system (Figs. 4B and 4C, respectively) or with relaxation (insets of Figs. 4B and 4C). It is shown that, in a free exciton system, the amount of coherence present in a significantly populated system strongly depends upon the excitation rate. Independently of the excited site (BChl 1 or 6), dynamical coherences are seen to be created only from ultra fast excitation (faster than $\sim 100 \text{ fs}^{-1}$), *i.e.* when the transfer time is shorter than the period of the coherent oscillations in the acceptor system. However, for slower feeding rate, typically 1 ps^{-1} , which is representative of the natural excitation received from the neighboring antennae [68, 69], the constant excitation of a site does not create any coherent superposition of excited states. Such behavior is entirely inhibited when considering the system in interaction with a bath, as shown by the insets of Figs. 4B and 4C.

Since excitation with feeding rates representative of the natural excitation (tens of picoseconds) does not lead to a superposition of coherent state already in a relaxation-free system, it is clear that the use of the Markovian dynamics does not limit the results. In other words, a system interacting with a slowly relaxing bath supporting non-Markovian evolution of excitons would, under excitation from neighboring antennae, also not lead to a coherent dynamics, which is in contrast with the concern recently raised in Ref. [53].

In our demonstration calculations, we have not treated non-secular effects. Recent experimental observations suggest that non-secular effects, through the coupling of population with coherence terms, could generate dynamical coherences [14]. It has been analytically shown [37] that non-secular effect could indeed be responsible for

coherent dynamics, but only in the very short transient interval time following excitation. Here, even if coherences would be created, the continuous excitation from the neighboring antennae would lead to destructive interferences and suppress any coherent superposition. The coherence is therefore lost before non-secular effects could potentially influence the energy transfer dynamics.

VI. CONCLUSIONS

The two different phenomena commonly referred to as coherence, namely the eigenstate delocalization and the dynamical quantum coherence, have mutually unrelated effects on the dynamics of electronic energy transfer in molecular aggregates. Coupling between spatially localized pigments leads to exciton delocalization which is thus an intrinsic property of a given molecular system. On the contrary, dynamic coherence appears only under special excitation conditions. The excitation of such coherence by means of light requires the interaction between the system and the light to be of short duration. Similarly, we find that the excitation of a coherent superposition of the antenna states by neighboring antennae requires two conditions. First, the rate of energy transfer from antenna to antenna should be large, so that the corresponding transfer time is shorter than the period of coherent oscillation in the acceptor antenna, and second, the population of donor state needs to be temporally limited to a short time interval.

Although statistical interpretation of quantum mechanics allows one to imagine the classical regime of incoherent hopping as a consequence of individual ultra fast hopping acts which would result in certain coherent superposition of states, it has to be stressed that it is the interpretation and not the underlying quantum theory that leads to this conclusion. No prescription is given by such interpretation about the time scale of the hopping events. On the contrary, when the well experimentally tested superposition principle of quantum mechanics is considered, as in decoherence theory, no hopping events in energy transfer and no coherent spikes in incoherent light can be justified. Consequently, no dynamical coherence can be expected under the usual excitation conditions found in nature.

The time evolution of the dynamical coherence generated by short excitation in photosynthetic systems can provide us with invaluable information about the internal dynamics of the photosynthetic energy transfer, and it can thus serve as an important diagnostic tool. However, the suggested significance of the dynamical coherence for natural light-harvesting cannot be currently experimentally confirmed, nor can it be theoretically expected based on the current understanding of quantum mechanics.

-
- [1] T. Förster, in *Modern Quantum Chemistry: Istanbul Lectures – Part III, Action of Light and Organic Crystals*, edited by O. Cinanogu (Academic, New York, 1965), Chap. Delocalized Excitation and Excitation Transfer, pp. 93–137.
- [2] R. Knox, in *Excitation energy transfer and migration: theoretical considerations*, edited by Govindjee (Academic, New York, 1975), pp. 183–221.
- [3] G. D. Scholes, *Annu. Rev. Phys. Chem.* **54**, 57 (2003).
- [4] S. Jang, Y.-C. Cheng, D. R. Reichman, and J. D. Eaves, *J. Chem. Phys.* **129**, 101104 (2008).
- [5] V. I. Prokhorenko, A. R. Holzwarth, F. R. Nowak, and T. J. Aartsma, *J. Phys. Chem. B* **106**, 9923 (2002).
- [6] G. S. Engel, T. R. Calhoun, E. L. Read, T.-K. Ahn, T. Mančal, Y.-C. Cheng, R. E. Blankenship, and G. R. Fleming, *Nature* **446**, 782 (2007).
- [7] H. Lee, Y.-C. Cheng, and G. Fleming, *Science* **316**, 1462 (2007).
- [8] T. R. Calhoun, N. S. Ginsberg, G. S. Schlau-Cohen, Y.-C. Cheng, M. Ballottari, R. Bassi, and G. R. Fleming, *J. Phys. Chem. B* **113**, 16291 (2009).
- [9] I. P. Mercer, Y. C. El-Taha, N. Kajumba, J. P. Marangos, J. W. G. Tisch, M. Gabrielsen, R. J. Cogdell, E. Springate, and E. Turcu, *Phys. Rev. Lett.* **102**, 057402 (2009).
- [10] E. Collini, C. Y. Wong, K. E. Wilk, P. M. G. Curmi, P. Brumer, and G. D. Scholes, *Nature* **463**, 644 (2010).
- [11] E. Harel and G. S. Engel, *Proc. Natl. Acad. Sci. U. S. A.* **109**, 706 (2012).
- [12] E. Collini and G. D. Scholes, *Science* **323**, 369 (2009).
- [13] D. B. Turner, R. Dinshaw, K. Lee, M. S. Belsley, K. E. Wilk, P. M. G. Curmi, and G. D. Scholes, *Phys. Chem. Chem. Phys.* **14**, 4857 (2012).
- [14] G. Panitchayangkoon, D. Hayes, K. A. Fransted, J. R. Caram, E. Harel, J. Wen, R. E. Blankenship, and G. S. Engel, *Proc. Natl. Acad. Sci. U. S. A.* **107**, 12766 (2010).
- [15] G. Panitchayangkoon, D. V. Voronine, D. Abramavicius, J. R. Caram, N. H. C. Lewis, S. Mukamel, and G. S. Engel, *Proc. Natl. Acad. Sci. U. S. A.* **108**, 20908 (2011).
- [16] A. Ishizaki and G. R. Fleming, *Proc. Natl. Acad. Sci. U. S. A.* **106**, 17255 (2009).
- [17] B. Hein, C. Kreisbeck, T. Kramer, and M. Rodríguez, *New J. Phys.* **14**, 023018 (2012).
- [18] T. Fujita, J. Huh, S. K. Saikin, J. C. Brookes, and A. Aspuru-Guzik, *ArXiv* **1304.4902**, (2013).
- [19] M. Mohseni, P. Rebentrost, S. Lloyd, and A. Aspuru-Guzik, *J. Chem. Phys.* **129**, 174106 (2008).
- [20] P. Rebentrost, M. Mohseni, I. Kassal, S. Lloyd, and A. Aspuru-Guzik, *New J. Phys.* **11**, 033003 (2009).
- [21] D. Hayes, G. Panitchayangkoon, K. A. Fransted, J. R. Caram, J. Wen, K. F. Freed, and G. S. Engel, *New J. Phys.* **12**, 065042 (2010).
- [22] A. Ishizaki and G. R. Fleming, *New Journal of Physics* **12**, 055004 (2010).
- [23] J. Wu, F. Liu, Y. Shen, J. Cao, and R. J. Silbey, *New J. Phys.* **12**, 105012 (2010).
- [24] D. Abramavicius and S. Mukamel, *J. Chem. Phys.* **134**, 174504 (2011).
- [25] J. Strümpfer and K. Schulten, *J. Chem. Phys.* **134**, 095102 (2011).
- [26] F. Caycedo-Soler, A. W. Chin, J. Almeida, S. F. Huelga, and M. B. Plenio, *J. Chem. Phys.* **136**, 155102 (2012).
- [27] J. R. Caram, N. H. C. Lewis, A. F. Fidler, and G. S. Engel, *J. Chem. Phys.* **136**, 104505 (2012).
- [28] D. Abramavicius and S. Mukamel, *J. Chem. Phys.* **133**, 064510 (2010).
- [29] A. G. Dijkstra, T. La Cour Jansen, and J. Knoester, *J. Chem. Phys.* **128**, (2008).
- [30] N. Christensson, H. F. Kauffmann, T. Pullerits, and T. Mančal, *J. Phys. Chem. B* **116**, 7449 (2012).
- [31] V. Tiwari, W. K. Peters, and D. M. Jonas, *Proc. Natl. Acad. Sci. U. S. A.* **110**, 1203 (2013).
- [32] A. Chenu, N. Christensson, H. F. Kauffmann, and T. Mančal, *Scientific Reports* to appear (2013).
- [33] Y.-C. Cheng and G. R. Fleming, *Annu. Rev. Phys. Chem.* **60**, 241 (2009).
- [34] X.-P. Jiang and P. Brumer, *J. Chem. Phys.* **94**, 5833 (1991).
- [35] P. Brumer and M. Shapiro, *Proc. Nat. Am. Soc.* **109**, 19575 (2012).
- [36] T. Mančal and L. Valkunas, *New Journal of Physics* **12**, 065044 (2010).
- [37] L. A. Pachón and P. Brumer, *ArXiv* 1210.6374v1 (2012).
- [38] A. Ishizaki and G. R. Fleming, *J. Phys. Chem. B* **115**, 6227 (2011).
- [39] E. A. Silinsh and V. Čápek, *Organic Molecular Crystals Interaction, Localization, and Transport Phenomena* (American Institute of Physics Press, ADDRESS, 1994).
- [40] H. van Amerongen, L. Valkunas, and R. van Grondelle, *Photosynthetic Excitons* (World Scientific, Singapore, 2000).
- [41] V. I. Novoderezhkin, M. A. Palacios, H. van Amerongen, and R. van Grondelle, *J. Phys. Chem. B* **109**, 10493 (2005).
- [42] N. Hashitsume, F. Shibata, and M. Shingu, *J. Stat. Phys.* **17**, 155 (1977).
- [43] F. Shibata, Y. Takahashi, and N. Hashitsume, *J. Stat. Phys.* **17**, 4 (1977).
- [44] R. Doll, D. Zueco, M. Wubs, S. Kohler, and P. Hanggi, *Chem. Phys.* **347**, 243 (2008).
- [45] T. Renger, V. May, and O. Kühn, *Physics Reports* **343**, 137 (2001).
- [46] R. van Grondelle and V. I. Novoderezhkin, *Phys. Chem. Chem. Phys.* **8**, 793 (2006).
- [47] V. May and O. Kühn, *Charge and Energy Transfer Dynamics in Molecular Systems* (Wiley-VCH, Berlin, 2001).
- [48] G. S. Engel, E. L. Read, T. R. Calhoun, T. K. Ahn, T. Mančal, R. E. Blankenship, and G. R. Fleming, in *Ultrafast Phenomena XV*, edited by P. Corkum, D. Jonas, R. J. D. Miller, and A. M. Weiner (Springer, Berlin, 2007), Vol. 88, pp. 392–394, 15th International Conference on Ultrafast Phenomena, Pacific Grove.
- [49] R. E. Blankenship, *Molecular Mechanism of Photosynthesis* (Blackwell Science, Oxford, 2002).
- [50] J. Olšina and T. Mančal, *J. of Mol. Modeling* **16**, 1765 (2010).
- [51] I. Barvik, V. Čápek, and P. Heřman, *J. Lumin.* **83-84**, 105 (1999).
- [52] I. Kassal, J. Yuen-Zhou, and S. Rahimi-Keshari, *J. Phys. Chem. L.* **4**, 362 (2013).
- [53] F. Fassioli, A. Olaya-Castro, and G. D. Scholes, *J. Phys. Chem. Lett.* **3**, 3136 (2012).

- [54] K. Hoki and P. Brumer, in *Procedia Chemistry* (Elsevier, 22nd Solvay Conference on Chemistry, 2011), Vol. 3, pp. 122–131.
- [55] S. Mukamel, *Principles of nonlinear spectroscopy* (Oxford University Press, Oxford, 1995).
- [56] R. Loudon, *The Quantum Theory of Light*, 3rd edition ed. (Oxford University Press, Oxford, 2000).
- [57] W. H. Zurek, Phys. Rev. D **26**, 1862 (1982), Decoherence, interesting model of apparatus.
- [58] J. P. Paz and W. H. Zurek, Phys. Rev. D **48**, 2728 (1993).
- [59] M. Schlosshauer, *Decoherence and the Quantum-to-Classical Transition* (Springer, Berlin, 2007).
- [60] R. Fenna and B. Matthews, Nature **258**, 573 (1975).
- [61] M. T. W. Milder, B. Brüggemann, R. van Grondelle, and J. L. Herek, Photosynth. Res. **104**, 257 (2010).
- [62] J. Adolphs and T. Renger, Biophys. J. **91**, 2778 (2006).
- [63] A. Ben-Shem, F. Frolow, and N. Nelson, FEBS lett. **564**, 274 (2004).
- [64] D. Tronrud, J. Wen, L. Gay, and R. Blankenship, Photosynth. Res. **100**, 79 (2009).
- [65] C. Olbrich, T. L. C. Jansen, J. Liebers, M. Aghar, J. Strümpfer, K. Schulten, J. Knoester, and U. Kleinekathöfer, J. Phys. Chem. B **115**, 8609 (2011).
- [66] J. Wen, H. Zhang, M. L. Gross, and R. E. Blankenship, Proc. Natl. Acad. Sci. U. S. A. **106**, 6134 (2009).
- [67] M. Sarovar, A. Ishizaki, G. R. Fleming, and K. B. Whaley, Nature Physics **6**, 462 (2010).
- [68] S. Savikhin, Y. Zhu, S. Lin, R. E. Blankenship, and W. S. Struve, J. Chem. Phys. **10322**, 10322 (1994).
- [69] J. Martiskainen, J. Linnanto, R. Kananavičius, V. Lehtovuori, and J. Korppi-Tommola, Chem. Phys. Lett. **477**, 216 (2009).